CONFERENCE PRE-PRINT

THE INTERACTION BETWEEN THE EDGE DISLOCATION AND THE DISLOCATION LOOP-BUBBLE COMPLEX UNDER SHEAR STRESS IN BCC IRON

Y.X. WEI, M. XU, L.P. GUO, N. GAO, W.P. ZHANG Southwestern Initute of Phypics Chengdu, China

Email: minxu_mx@fudan.edu.cn; guolp@whu.edu.cn

Abstract

In advanced nuclear reactors, structural materials are subjected to stress, leading to dislocation slip. Understanding the interaction between dislocation slip and irradiation-induced defects is crucial for the practical application of nuclear structural materials. Currently, studies on the interaction between dislocations and dislocation loop-H-bubble complexes remain limited. In this study, molecular dynamics simulations were employed to investigate the interaction of edge dislocations with three forms of dislocation loop-H-bubble complexes: with the H bubble inside the loop (C1), at the upperedge dislocation core (C2), and at the lower-edge dislocation core (C3). The results show that these complexes significantly hinder dislocation slip. The critical resolved shear stress (CRSS) values required for an edge dislocation to overcome complexes C1, C2 and C3 are 120, 90 and 225 MPa, respectively. The hindering strength is primarily determined by the H bubble and strongly depends on its position within the complex. During the interaction, part of the dislocation loop is absorbed by the dislocation, rendering the loop itself a relatively minor contributor to the overall pinning effect.

1. INTRODUCTION

In the advanced nuclear reactor, the structural materials need to provide sufficient mechanical support for the reactor device [1]. In a state of stress for a long time, the shear force acting on the crystal for a long time causes it to deform, which affects the mechanical properties of the material. Under the influence of shear stress, crystals deform through plastic deformation (elastic deformation) or uniform deformation (homogeneous deformation). In the crystal, the main way in which plastic deformation occurs is through the slip of dislocations. Dislocation slip is characterized by the displacement of a crystal in a specific crystallographic direction (called a slip direction) and a specific lattice plane (called a slip plane). Steps are created on the crystal surface during dislocation slip, which indicates the inhomogeneity of the slip process. The slip of dislocations in the lattice requires external stress to drive it. To activate a dislocation slip, it's necessary to have a minimum stress value that is known as the Peierls-Nabarro force [2, 3]. The value of the Peierls-Nabarro force is generally low. For example, in BCC iron, the Peierls-Nabarro force is about 25 MPa [4]. Thus, it can be observed that dislocation slip in the material can easily be activated. However, there will be a large number of defects in the irradiated materials. The movement of dislocations can be hindered by defects when they come into contact with each other, which directly affects the deformation mechanism of the material. Understanding the interaction between dislocations and various defects is very meaningful work for the practical application of nuclear structural materials.

For the interaction between dislocations and dislocation loops, Osetsky et. al. [5-7] reported that dislocation loops in the matrix can suppress the mobility of dislocations. The strength of the pinning is mainly related to the type, size, number density and Burg vector of the dislocation loops. Dislocation loops impede the movement of dislocations mainly through direct contact or elastic interaction, resulting in an increase in the material's yield stress and a decrease in ductility, a phenomenon known as "hardening"[8-9]. For the interaction between dislocation and vacancy defects, the dislocation tends to intermix with vacancy clusters. Because the strain energy of the dislocation core in the inner part of the cavity is zero. Under sufficient shear force, dislocations can be released from pinning of vacancies by climbing. Similarly, the presence of bubbles in the matrix can also hinder the movement of dislocations. In BCC iron, the hindering intensity of helium bubbles to the dislocations is slightly higher than that of corresponding sized voids, and it decreases with increasing temperature [10-13].

We have previously investigated the interaction between dislocation loops and H-bubbles in BCC iron, found that, dislocation loops and H-bubbles can form the morphology of a loop-bubble complex under certain conditions [14]. A similar structure of loop-bubble complexes in BCC iron-based alloys has also been observed experimentally [15-17]. This paper primarily employs molecular dynamics to investigate the pinning behavior

of dislocation loop-H-bubble complexes on edge dislocations. In BCC iron, dislocation slip occurs along the <111> direction, with the corresponding Burgers vector of (a0/2)[111], and includes two types of edge dislocations: 1/2<111>{112} and <111>{011} [14]. In this study, 1/2<111>{112} type edge dislocations are selected as the focus, and the loop-bubble complexes are modeled using interstitial 1/2<111> dislocation loops with embedded H bubbles.

In addition, in BCC iron and its alloy materials, there are many studies about interaction between bubbles and dislocations was mainly focus on He bubbles[10-13], while the related research on the interaction between H bubbles and dislocations was relatively lack. Furthermore, numerous studies have investigated the interaction between dislocation loops and dislocations [5-7]. Therefore, before carrying out the simulation of the interaction between the loop-bubble complex and the edge dislocation, we first calculated the hindering behavior of the H-bubble on the edge dislocation, so as to be able to better understand and compare the interaction between the loop-bubble complex and the edge dislocation.

2. SIMULATION METHODS

In this work, an embedded atom method (EAM) potential function developed by Ramasubramaniam et. al. [18] was applied to describe the Fe-H interaction. The portion of this potential function describing the Fe-Fe interaction is based on the potential published by Ackland et. al. [19]. This Ackland potential is excellent in describing the behavior of dislocations in BCC iron, and its calculated results are basically consistent with the first-principles results, which are very suitable for calculating the interaction between dislocations and irradiation defects. The calculation box as shown in Fig. 1. Periodic boundary conditions are applied in both the x-direction and the z-direction of the computational cell.

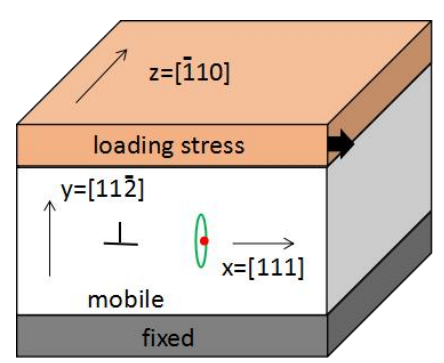


FIG. 1. Schematic diagram of the calculation box. The orange region represents the top surface atomic layer, the gray region represents the bottom surface atomic layer, and the white region in the middle represents the internal atomic layers of the matrix.

To better understand the properties of the dislocation loop-H bubble complex, we first simulate the interaction between an H bubble and an edge dislocation, considering bubble sizes of 1 nm, 2 nm and 3 nm, and H/V ratios in the range of 0 - 0.8. Based on these results, we then calculate the interaction between the dislocation loop-bubble complex and an edge dislocation. As shown in Fig. 2, three forms of dislocation loop-H bubble complexes (labeled C1, C2, and C3) are considered.

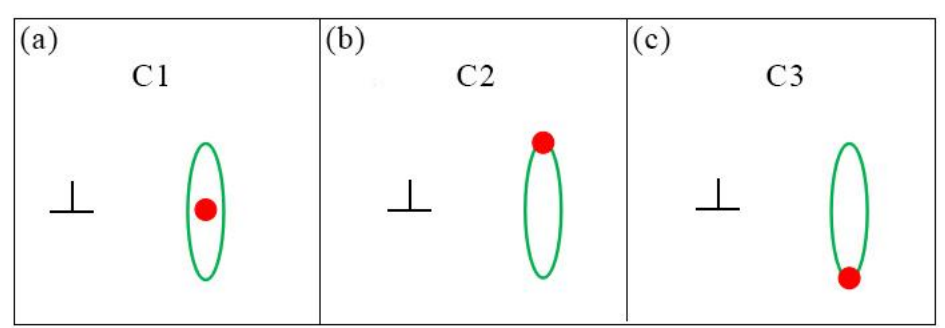


FIG. 2. Schematic diagram of the initial relative positions between the edge dislocation and the three types of dislocation loop-H bubble complexes in the simulation. (a) The H bubble is located inside the dislocation loop, without contact with the dislocation core at the edge, labeled as C1; (b) The H bubble is located at the dislocation core on the upper edge of the dislocation loop, labeled as C2; (c) The H bubble is located at the dislocation core on the lower edge of the dislocation loop, labeled as C3.

3. RESULTS

3.1. Interaction between edge dislocations and H bubbles

Fig. 3 summarizes the critical resolved shear stress (CRSS) values for 1/2<111>{112} edge dislocations passing through H bubbles of different sizes and H/V ratios, where the bubble sizes are 1 nm, 2 nm and 3 nm, and the H/V ratio ranges from 0 to 0.8. In single crystal, the resistance strength of various defects to dislocation slip is mainly reflected by CRSS value. The CRSS value refers to the minimum shear stress value required to overcome the pinning effect when the dislocation crosses the obstacle. It is found that as the size of the H bubble is larger, the pinning effect is stronger. Dislocations pass through H bubbles in the same way as through voids (both climb and cut through).

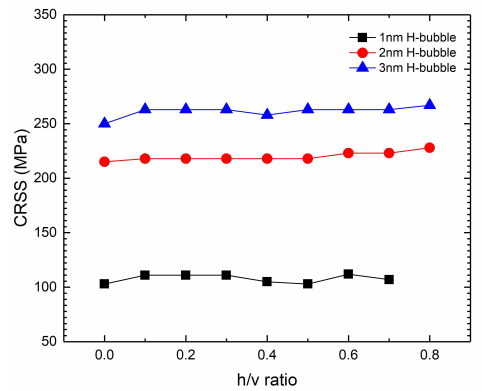


FIG. 3. Variation of the CRSS with increasing H/V ratio inside the H bubble. The bubble sizes are 1 nm, 2 nm and 3 nm.

3.2. Interaction between edge dislocations and dislocation loop-H-bubble complexes

Fig. 4 shows the detailed process of the interaction between the 1/2<111>{112} edge dislocation and the loop-bubble complex C1 under shear stress conditions.

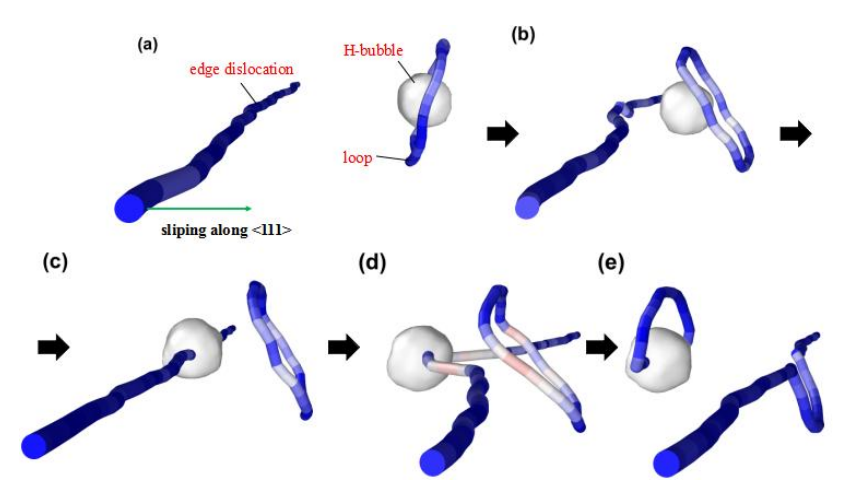


FIG. 4. Schematic of the dynamic interaction process between an edge dislocation and the loop-bubble complex C1. Panels (a)-(e) show the evolution of the dislocation and the loop-bubble complex at different stages in terms of shape and relative position. The blue segments of the dislocation represent edge dislocation portions, while the pinkish-white segments indicate regions approaching a screw dislocation character, which generally occurs when segments of the dislocation are strongly pulled or twisted. The gray spheres represent the H bubble.

Fig. 4(a) shows the state of dislocations and loop-bubble complexes after the entire system is relaxed in an unstressed state. In order to confirm that the dislocation loop and the H bubble indeed form a relatively stable complex, the entire stress-free relaxation process lasted for 20 ps, during which the loop-bubble complex presented a stable state, and the H bubble was always located inside the dislocation loop, no contact with dislocation core. After shear stress is applied, the dislocation evolution, beginning with slip and ending with the complete unpinning of the loop-bubble complex, occurs in three distinct stages. In the first stage, as shown in Fig. 4(b), after the dislocation slip reaches the vicinity of the loop-bubble complex, the dislocation and the loop-bubble complex show the short-ranged repulsion. The middle bending state of the dislocation and the rightward

shift of the dislocation loop, indicate that the dislocation and the loop-bubble complex exhibit mutual repulsion, which mainly originates from the elastic interaction between the dislocation and the dislocation loop. At this point, the dislocation encounters the first obstacle, and the slip action stops. In the second stage, the shear stress strength is increased, and the dislocations overcome the resistance and continue to move forward. As shown in Fig. 4(c), the dislocation continues to slip forward, the dislocation loop is pushed away from the bubble, and the loop-bubble complex morphology is disrupted. The dislocation slips to the hydrogen bubble. The interaction between the dislocation and the bubble preventing dislocation from strengthening again. In the third stage, the shear stress strength is increased again, and the dislocation are pulled into a curved state by the pinning action of the bubble and the drive of the shear stress, as shown in Fig. 4(d). Interestingly, because the dislocation loop is attracted by the H bubble, it still stays in the vicinity of the H bubble. At the same time, the dislocation gradually approached the edge of the dislocation loop. When the two are in contact, the dislocation absorbs half of the dislocation loop, and this half of the dislocation loop forms a super-jog-like dislocation segment on the dislocation line, as shown in Fig. 4(e). The newly formed dislocation with super-jog-like dislocation segments no longer intersect with the bubbles, so the dislocation are unpinned and continue to slide forward. The remaining half of the dislocation loop is attracted by the bubble, and the two re-form a new loop-bubble complex. The critical resolved shear stress (CRSS) required for an edge dislocation to overcome the barrier of the loop-bubble complex C1 is 120 MPa.

Fig. 5 shows the interaction of edge dislocations with loop-bubble complex C2 under shear stress. In the loopbubble complex, the H bubble is located at the upper edge of the dislocation loop. Fig. 5(a) shows the initial state of dislocation and complex C2 after the system is relaxed in the unstressed state. It can be seen that the dislocation-to-dislocation loop repulsion has caused the unpinned part of the dislocation loop in complex C2 to shift to the right. As shown in Fig. 5(b), after applying shear stress, as the dislocation approaches the complex C2, the middle part of the dislocation also bends under the repulsive effect. Increase the shear stress value until the dislocation hits the edge of the dislocation loop. As shown in Fig. 5(c), when the dislocation just touches the edge of the dislocation loop, the instantaneous form of the dislocation, the dislocation loop and the hydrogen bubble is mixed together. In order to show more clearly, the top view of the middle hybrid part is given in Fig. 5(e). Since the dislocation and the dislocation loop are integrated, we use black lines to outline the part originally belonging to the dislocation loop and the part belonging to the edge dislocation respectively in the figure. The contact point position between the dislocation and the edge of the dislocation loop is marked with a red circle. When point A on the edge dislocation in the figure touches point B on the other side of the dislocation loop, the dislocation absorbs the lower half of the dislocation loop, forming a super-jog-like dislocation segment, as shown in Fig. 5(d). There is no obstacle on the super-jog-like dislocation segment which can continue to slip. The corresponding CRSS value is 90Mpa. The original complex C2 remained in place as a new complex after losing half of the dislocation loop.

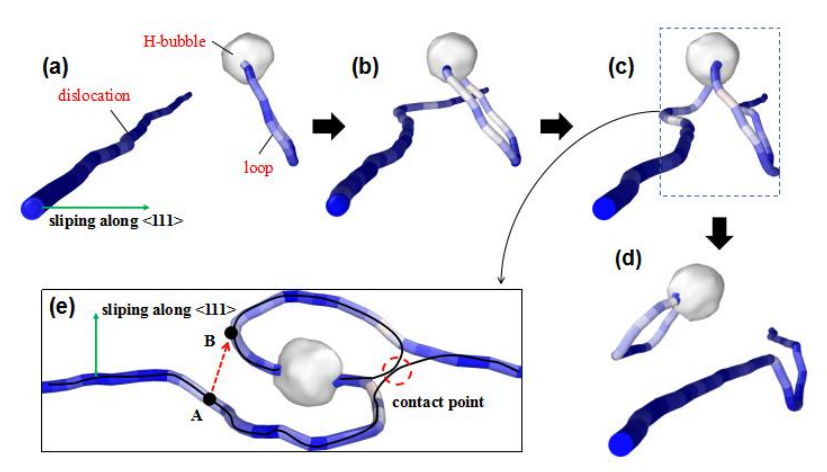


FIG. 5. Schematic of the dynamic interaction process between an edge dislocation and the loop-bubble complex C2. Panels (a)-(d) show the evolution of the dislocation and the loop-bubble complex at different stages in terms of shape and relative position. (e) shows a top view of the structure within the dashed box in (c). The blue segments of the dislocation represent edge dislocation portions, while the pinkish-white segments indicate regions approaching a screw dislocation character. The gray spheres represent the H bubble.

Fig. 6 shows the interaction of edge dislocations with loop-bubble complex C3 under shear stress. At this part, the H bubble is located at the lower edge of the dislocation loop in the complex. The initial state of the dislocation and the complex C3 after the system is relaxed in the unstressed state. As shown in Fig. 6(b)-(c), the dislocation is driven by shear stress to approach and absorb the dislocation loop in the lower half of the C3

complex, which forms a bulge-like dislocation segment (super-jog). The super-jog contains the hydrogen bubble(2nm) in the original complex C3. Therefore, the new dislocation that have absorbed part of the dislocation loop must continue to overcome the H-bubble. As shown in Fig. 6(d) is the critical state before the dislocation breaks free from H-bubble pinning. At this time, the two dislocation lines near the H bubble have temporarily turned into screw dislocations under the pulling action. After the dislocation breaks free from the pinning of the H-bubble, as shown in Fig. 6(e), there is also a small protrusion in the middle of the bulge-like dislocation segment (super-jog) of the dislocation, indicating that the dislocation is by climbing the way to cross the H-bubble pinning. The corresponding CRSS value is about 225Mpa. At this time, the original dislocation loop-bubble complex C3 has disintegrated after the dislocation is drawn. The hydrogen bubbles stay in place alone, half of the dislocation loop is absorbed by the dislocation, and the other half of the small dislocation loop is formed in the matrix.

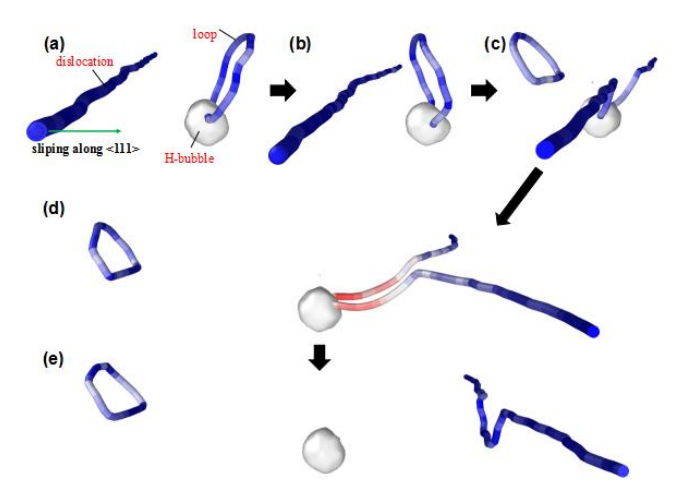


FIG. 6. Schematic of the dynamic interaction process between an edge dislocation and the loop-bubble complex C3. Panels (a)-(e) show the evolution of the dislocation and the loop-bubble complex at different stages in terms of shape and relative position. The blue segments of the dislocation represent edge dislocation portions, while the pinkish-white segments indicate regions approaching a screw dislocation character. The gray spheres represent the H bubble.

4. DISCUSSION

As shown in Fig. 3, the CRSS value increases significantly with increasing H-bubble size. The pinning strength of 2nm bubbles to dislocations is directly more than twice that of 1nm bubbles, while the increase in pinning strength of 3nm bubbles is smaller. The effect of size effect on the CRSS value is very strong. However, with the increase of the H/V ratio in the H bubble, the CRSS value just has a slight upward trend. When H/V equals 0, it corresponds to a void. The pinning strength of H bubbles to dislocations is almost equivalent to that of voids of the same size. The simulation results indicate that the hindering strength of H bubbles and voids to dislocation slip is comparable and their interaction behaviors with edge dislocations are very similar, consistent with the Orowan mechanism of dislocation bypassing non-penetrable obstacles such as precipitates and voids in BCC iron.

Fig. 3 shows that an H bubble with a size of 2 nm and H/V = 0.7 exerts a barrier strength of 223 MPa on edge dislocations, while the CRSS for an edge dislocation to overcome the loop-bubble complex C1 is only 120 MPa, indicating that the pinning effect of the C1 complex is substantially weaker than that of a single H bubble. Combining the characteristics of the interaction between bubbles/dislocation loops and edge dislocations, we summarize the main interactions involved in the interaction between dislocations and complex C1 into the following points: (1) The pinning effect of hydrogen bubbles on 1/2<111> dislocation loops and the elastic repulsion between dislocation loops and dislocations are the main reasons why the loop-bubble complex can be an obstacle to the movement of dislocations. At this time, the repulsion between dislocations and dislocation loops is stronger than the attraction of H bubbles to dislocations. (2) As the shear stress increases, the dislocation continues to approach the complex, while the complex disintegration due to elastic stress field between dislocation loop nearby. The dislocation loop at this time shows a pulled shape as shown in Fig. 4(d). The pulling force acting on the dislocation loop comes from both of the repulsive force of the dislocation and the attraction of shear stress, once it touches the dislocation loop, the dislocation line can absorb half of the

IAEA-CN-336/INDICO 3366

dislocation loop to form a super-jog-shaped dislocation segment. Since the dislocation core at the edge of the dislocation loop is not connected to the H bubble, the super-jog-like dislocation segment just helps the dislocation bypass the pinning of the H bubble. Therefore, 120Mpa corresponds to the stress value when the dislocation just touches the dislocation loop. Of course, it is much smaller than the corresponding 223Mpa when the dislocation line is pulled to break free from the H bubble. (4) After the dislocation crosses the hydrogen bubble and the dislocation loop shrunk by half, the dislocation loop is no longer subject to the repulsive force from the dislocation, so the loop is re-synthesized into a new complex stays in the initial position under the attraction of the H bubble.

During the interaction between the dislocation and C2, since the H bubble is located at the dislocation core, it exerts a stronger pinning effect on the dislocation loop compared with C1. Therefore, when the dislocation begins to approach C2 under applied shear stress, the elastic repulsion between the dislocation and the dislocation loop causes only a positional shift of the loop, without detaching it from the dislocation loop-H bubble complex. As the shear stress continues to increase, the dislocation comes into contact with and merges into the dislocation loop of C2, after which it absorbs the lower half of the loop and detaches from C2. In this process, the H bubble does not directly participate in hindering the dislocation slip, and thus the CRSS value of 90 MPa is smaller than the CRSS value of 223 MPa for the interaction between the H bubble and the dislocation.

The interaction process between the dislocation and C3 is similar to that between the dislocation and C2. When the dislocation approaches C3, the elastic repulsion between the dislocation and the dislocation loop causes a positional shift of the loop. It is worth noting that this repulsive force mainly acts on the lower half of the dislocation loop, and in addition, the pinning of the H bubble also acts on the lower part of the loop. Therefore, during the approach of the dislocation, the positional shift of the dislocation loop in C3 is smaller compared with the interaction processes with C1 and C2, resulting in a more stable loop-bubble complex than C1 and C2. Differently from the interaction with C2, as the shear stress continues to increase, when the dislocation comes into contact with the dislocation loop at C3, it absorbs both the lower half of the dislocation loop and the H bubble located in the lower part of C3. In this case, the dislocation slip is entirely hindered by the H bubble, and thus the CRSS value of 225 MPa is close to the 223 MPa CRSS value for the interaction between the H bubble and the dislocation.

The results of the interactions between edge dislocations and complexes C1, C2 and C3 show that the loop-bubble complex indeed hinders dislocation slip, and that the position of the bubble within the loop significantly influences the blocking strength of the complex. The CRSS values indicate that the blocking strengths of the three loop-bubble complexes against edge dislocations are arranged as C2 (90Mpa) < C1 (120Mpa) < C3 (225Mpa). In summary, C2 is the weakest obstacle to the edge dislocation, because in the process of unpinning the dislocation, it only needs to overcome the repulsion between it and the dislocation loop. The pinning effect can be released as soon as it contacts the dislocation loop. C1 is generally a hindrance to edge dislocations. In the process of unpinning the dislocation, it needs to be pinned by the H bubble, and the pinned dislocation can be unpinned by contacting the dislocation ring after the pulled dislocation segment. C3 is the strongest barrier to edge dislocations. After dislocation absorbs the dislocation loop, since the H bubble is located at the edge of the half of the dislocation loop absorbed by the dislocation, the dislocation loop must be in the shear stress. Drive the pinning directly across the H-bubble. Therefore, the hindering strength of dislocations by C3 (~225Mpa) is similar to that of a single H-bubble in C3 (~223Mpa). The above differences in pinning strength are caused by the different positions of the H bubbles in the composite. The number and size of H bubbles on the dislocation cores of the dislocation loop determine the strength of the loop-bubble complex in hindering dislocation slip.

In addition, numerous works have already performed detailed simulations of the interaction between edge dislocations and 1/2<111> interstitial dislocation loops using molecular dynamics methods [4, 21-24]. The results show that when a dislocation encounters a dislocation loop, it is very easy to absorb part or all of the dislocation loop to form a super-jog-like dislocation segment. However, when the edge dislocation slip plane is parallel to the dislocation loop Burg vector, it is difficult for the dislocation to contact the dislocation loop. This is due to the elastic repulsion between the dislocations and the strong mobility of the 1/2<111> interstitial dislocation loops when the dislocations slip toward the dislocation loops. When the dislocation is close to the 1/2<111> dislocation loop, the repulsive force between the two will make the 1/2<111> dislocation loop move away quickly, so it is difficult for the two to make direct contact. In our constructed model, the interaction between a 1/2<111> edge dislocation and a 1/2<111> interstitial dislocation loop was also calculated, yielding a corresponding CRSS of 65 MPa.

Table 1 summarizes the hindering of dislocation slip by 1/2 < 111 > dislocation loops, H bubbles and the three types of dislocation loop-H bubble complexes. A comparison reveals that: (1) The existence of the bubble can

improve the hindering strength of dislocation loop to dislocation. The single 1/2<111> dislocation loop has almost no hindering effect on dislocation slip due to its easy migration. However, the addition of H bubbles can pin the 1/2<111> dislocation loop, making the dislocation. The elastic force field between the loop and the dislocation can hinder the slip of the dislocation to a certain extent. (2) The existence of dislocation loops will weaken the pinning strength of H bubbles on the slip surface to dislocations, but it can expand the range of H bubbles on the non-slip surface that hinder dislocations. (3) The existence of shear stress can reduce the size of the loop-bubble complex through dislocation slip, and may even directly disintegrate the structure of the loop-bubble complex and restore it to a separate dislocation ring and H-bubble structure.

TABLE 1. SUMMARY OF THE HINDRANCE TO DISLOCATION SLIP CAUSED BY 1/2 <111> DISLOCATION LOOPS, H-BUBBLES AND THREE TYPES OF DISLOCATION LOOP-BUBBLE COMPLEXES.

	Loop	C1	C2	С3	H bubble
Initial state	_ ()	⊥ •	⊥ (т ()	⊥ •
Final state				_	•
CRSS	65 MPa	120 MPa	90 MPa	225 MPa	223 MPa
Interaction force without external stress	Repulsive force	Repulsive force	Repulsive force	Repulsive force	Attractive force
Main source of resistance	Loop	H-bubble	Loop	H-bubble	H-bubble
Depinning mechanism	No pinning effect	During the pinning process by H bubbles, part of the loops are absorbed while others bypass them.	Overcoming the repulsive force of loops, part of the dislocation loops are absorbed.	Climb	Climb

5. CONCLUSION

In this study, molecular dynamics simulations were employed to investigate the hindering effect of H bubbles with different sizes and H/V ratios on edge dislocations in BCC iron. The results indicate that the bubble size has a pronounced influence on the pinning strength against dislocations, whereas variations in the H/V ratio exert only a minor effect. The pinning strength of H bubbles is comparable to that of cavities of the same size, and the mechanism by which edge dislocations bypass H bubbles is consistent with the Orowan mechanism.

Subsequently, the effects of three forms of dislocation loop-H-bubble complexes on the migration behavior of edge dislocations are examined: C1, with the H bubble inside the loop; C2, with the H bubble at the upper-edge

IAEA-CN-336/INDICO 3366

dislocation core; and C3, with the H bubble at the lower-edge dislocation core. The results reveal that these complexes significantly hinder dislocation slip. The CRSS values required for an edge dislocation to overcome complexes C1, C2 and C3 are 120, 90 and 225 MPa, respectively. The hindering strength mainly arises from the H bubble and is strongly influenced by its position within the complex. During the interaction, part of the dislocation loop is absorbed by the dislocation, so its contribution to hindering dislocation slip is relatively minor.

REFERENCES

- [1] S.J. Zinkle, J.T. Busby, Structural materials for fission & fusion energy, Materials Today 12 (2009) 12-19.
- [2] R. Peierls, The size of a dislocation, Proceedings of the Physical Society 52 (1940) 34-37.
- [3] F.R.N. Nabarro, Dislocations in a simple cubic lattice, Proceedings of the Physical Society 59 (1947) 256-272.
- [4] Y.N. Osetsky, D.J. Bacon, An atomic-level model for studying the dynamics of edge dislocations in metals, Modelling & Simulation in Materials Science & Engineering 11 (2003) 427-446.
- [5] K. Tapasa, D.J. Bacon, Y.N. Osetsky, Computer simulation of dislocation-solute interaction in dilute Fe-Cu alloys, Modelling & Simulation in Materials Science & Engineering 14 (2006) 1153–1166.
- [6] D. Terentyev, D.J. Bacon, Y.N. Osetsky, Interaction of an edge dislocation with voids in α-iron modelled with different interatomic potentials, Journal of Physics Condensed Matter 20 (2008) 445007.
- [7] D. Terentyev, P. Grammatikopoulos, D.J. Bacon, Y.N. Osetsky, Simulation of the interaction between an edge dislocation and a <1 0 0> interstitial dislocation loop in α-iron, Acta Materialia 56 (2008) 5034-5046.
- [8] Y.N. Osetsky, R.E. Stoller, Y. Matsukawa, Dislocation-stacking fault tetrahedron interaction: What can we learn from atomic-scale modelling, Journal of Nuclear Materials (2004) 1228-1232.
- [9] M. Victoria, N. Baluc, C. Bailat, Y. Dai, M.I. Luppo, R. Schäublina Aublin, B.N. Singh, The microstructure and associated tensile properties of irradiated fcc and bcc metals, Journal of Nuclear Materials 276 (2000) 114-122.
- [10] D. Hull, D.J. Bacon. Introduction to Dislocations. 2011, 14(10):502.
- [11] R. Schäublin, Y.L. Chiu, Effect of helium on irradiation-induced hardening of iron: A simulation point of view, Journal of Nuclear Materials 362 (2007) 152-160.
- [12] S.M. Hafez Haghighat and R. Schaeublin, Molecular dynamics modeling of cavity strengthening in irradiated iron, Proceedings of Third International Conference of Multiscale Materials Modeling, Freiburg, Germany, September 2006, p.729.
- [13] S.M.H. Haghighat, R. Schaeublin, Molecular dynamics modeling of cavity strengthening in irradiated iron, Journal of Computer-Aided Materials Design 14 (2007) 191-201.
- [14]
- [15] S.M. Hafez Haghighat, R. Schaublin, Influence of the stress field due to pressurized nanometric He bubbles on the mobility of an edge dislocation in iron, Philosophical Magazine 90 (2010) 1075-1100.
- [16] J. Chen, P. Jung, W. Hoffelner, H. Ullmaier, Dislocation loops and bubbles in oxide dispersion strengthened ferritic steel after helium implantation under stress, Acta Materialia 56 (2008) 250-258.
- [17] D. Brimbal, B. Décamps, A. Barbu, E. Meslin, J. Henry, Dual-beam irradiation of α-iron: Heterogeneous bubble formation on dislocation loops, Journal of Nuclear Materials 418 (2011) 313-315.
- [18] A. Ramasubramaniam, M. Itakura, E.A. Carter, Interatomic potentials for hydrogen in α -iron based on density functional theory, Physical Review B 79 (2009) 174101.
- [19] G.J. Ackland, M.I. Mendelev, D.J. Srolovitz, S. Han, A. V. Barashev, Development of an interatomic potential for phosphorus impurities in α-iron, Journal of Physics Condensed Matter 16 (2004) S2629-S2642.
- [20] G. Monnet, D. Terentyev, Structure and mobility of the 1/2< 1 1 1 > {1 1 2} edge dislocation in BCC iron studied by molecular dynamics, Acta Materialia 57 (2009) 1416-1426.
- [21] A. Nomoto, N. Soneda, A. Takahashi, S. Ishino, Interaction Analysis between Edge Dislocation and Self Interstitial Type Dislocation Loop in BCC Iron Using Molecular Dynamics, Materials Transactions46 (2005) 463-468.
- [22] Z. Rong, Y.N. Osetsky, D.J. Bacon, A model for the dynamics of loop drag by a gliding dislocation, Philosophical Magazine 85 (2005) 1473-1493.
- [23] D.J. Bacon, Y.N. Osetsky, Z. Rong, Computer simulation of reactions between an edge dislocation and glissile self-interstitial clusters in iron, Philosophical Magazine 86 (2006) 3921-3936.
- [24] D. Terentyev, L. Malerba, D.J. Bacon, Y. Osetsky, The effect of temperature and strain rate on the interaction between an edge dislocation and an interstitial dislocation loop in α-iron, Journal of Physics Condensed Matter19 (2007) 456211.